33RD CONGRESS
OF THE INTERNATIONAL COUNCIL
OF THE AERONAUTICAL SCIENCES
STOCKHOLM, SWEDEN, 4-9 SEPTEMBER, 2022

ICAS 2022 SWEDEN

# NONLINEAR VIBRATION-BUCKLING INVESTIGATION OF UNSTIFFENED AND STIFFENED STRUCTURES SUBJECTED TO MECHANICAL AND THERMAL LOADINGS

Azzara R.[1*], Filippi M.[1], Pagani A.[1] & Carrera E.[1]

[1]MUL[2], Department of Mechanical and Aerospace Engineering
Politecnico di Torino

## Abstract

This works intend to present a novel numerical approach for carrying out virtual Vibration Correlation Technique (VCT) in stiffened and unstiffened structures subjected to mechanical and thermal loadings in order to predict the buckling load, to characterize the natural frequencies variation for progressively increasing loads, and to provide a verification of the experimental VCT results. The study has been performed using the well-established Carrera Unified Formulation (CUF) able to describe several kinematic models for one-dimensional (1D) and two-dimensional (2D) structures. All Green-Lagrange strain components are employed because far nonlinear regimes are investigated. Furthermore, the geometrical nonlinear equations are written in a total Lagrangian framework and solved with an opportune Newton-Raphson method along with a path-following approach based on the arc-length constraint. Different structures have been investigated and compared with the Abaqus solution in order to validate the proposed approach and provide some benchmark solutions. The results document the good accuracy and reliability of the proposed approach and show this numerical tool's potentialities. The virtual VCT can be used effectively during the preparation of experimental tests in order to appropriately investigate the boundary conditions to be applied or it can be a powerful method to be used to investigate cases that are difficult to analyze experimentally, such as structures subjected to thermal or shear loads.

**Keywords:** VCT; Natural frequencies; Buckling; Geometrical nonlinearity; Thermal loadings.

## 1. Introduction

One of the most important important experimental methods used in aerospace industry for the assessment of the buckling is the Vibration Correlation Technique (VCT) [1,2]. This nondestructive experimental test allows to calculate the buckling load and the equivalent boundary conditions by interpolating the natural frequencies of the structures for progressively increasing applied loads without reaching instability. The first experimental VCT investigations were performed by Lurie [3], Meier [4] and Chu [5]. In view of its importance and potential, several experimental tests and studies were carried out for decades. Recently, Abramovich et al. [6] adopted the VCT to evaluate the buckling load of metallic and laminated structures. Jansen et al. [7] presented the capability of analysis tools for supporting and improving the accuracy of the VCT results obtained through semi-empirical methods. For the sake of brevity, readers are referred to [8,9] for further detailed investigations. The literature on VCT analyses of isotropic and classical composite one-dimensional (1D) and two-dimensional (2D) structures is vast [10,11]. However, in practical industrial applications, this method exhibits some limitations due to complicated boundary conditions or particular types of loading, such as thermal. The principal goal of this work is to overcome these limitations and provide an efficient methodology based on high-accuracy but efficient layerwise (LW) models to investigate the dynamic characteristics of unstiffened and stiffened metallic and composite beam, plate and shell structures under extreme compressive and thermal loadings. This approach presents a powerful

methodology to study cases that are difficult to investigate experimentally, such as structures subjected to thermal or shear loads and with complicated boundary conditions, among others.
In this context, the structures are formulated in the Carrera Unified Formulation (CUF) [12] framework in order to obtain accurate results. The main advantage of the CUF is to be able to consider the structural model order as an input of the analysis. In this way, the refined generic models do not need specific formulations. One of the advantages of the present formulation with respect to the others, often based on linear approaches, is to consider the geometrical nonlinearities that allow to guarantee a remarkable accuracy of the results. In fact, the nonlinear governing equations and the relative finite element (FE) arrays of the 2D theories are written in terms of Fundamental Nuclei (FNs). FNs represent the basic building blocks of the presented formulation. The investigated structures are subjected to progressively higher applied loads, and for each state of equilibrium, on the deformed structure, the natural frequencies are calculated by solving a linearized eigenvalue problem, obtained from an analysis of the free vibration on the structure.

## 2. Vibration around nonlinear equilibrium states

The application of the presented methodology to investigate the vibration around nonlinear equilibrium states can be described in the following steps: 1) first, the static geometrical nonlinear problem is solved using the Newton-Raphson method based on the arc-length approach; 2) Once the nonlinear equilibrium is computed, the tangent stiffness matrix $\boldsymbol{K}_T$ is obtained in each states of interest; 3) Then, since the modal behavior of a structure is not a property of the geometric and mechanical characteristics, but it is a property of the state of equilibrium, the free vibrations analysis is carried out around a linearized (non-trivial) equilibrium state along the nonlinear path. Namely, the linearization of the equation of motion is written as:

$$\delta(\delta L_{int} + \delta L_{ine} - \delta L_{ext}) = \delta \boldsymbol{q}_{sj}^T \boldsymbol{K}_T^{ij\tau s} \delta \boldsymbol{q}_{\tau i} + \delta \boldsymbol{q}_{sj}^T \boldsymbol{M}^{ij\tau s} \delta \ddot{\boldsymbol{q}}_{\tau i} \tag{1}$$

where $\boldsymbol{M}^{ij\tau s}$ is the FN of the mass matrix and it is assumed to be linear, $\boldsymbol{K}_T^{ij\tau s}$ represents the FN of the tangent stiffness matrix and $\boldsymbol{q}_{\tau i}$ indicates the vector of the unknown nodal variables. 4) By assuming harmonic motion around non-trivial equilibrium states, the equation of motion is simplified into a linear eigenvalues problem, Eq. (2), from which it is possibile to evaluate natural frequencies and mode shapes.

$$\left(\boldsymbol{K}_T^{ij\tau s} - \omega^2 \boldsymbol{M}^{ij\tau s}\right) \delta \tilde{\boldsymbol{q}}_{\tau i} = 0 \tag{2}$$

in which ω indicates the natural frequencies and $\delta \tilde{\boldsymbol{q}}_{\tau i}$ is the eigenvector. If the full nonlinear tangent stiffness matrix is considered the method is called full nonlinear approach, whereas in the case of small rotations and linear pre-buckling, $\boldsymbol{K}_T^{ij\tau s}$ can be approximated as the sum of the linear stiffness $\left(\boldsymbol{K_0} = \boldsymbol{K}_S(q=0)\right)$, with $\boldsymbol{K}_S$ the secant stiffness matrix, and the geometric (pre-stress) contribution $\boldsymbol{K}_\sigma$,

$$\boldsymbol{K}_T \approx \boldsymbol{K}_0 + \boldsymbol{K}_\sigma \tag{3}$$

This expression of $\boldsymbol{K}_T$ is valid around the trivial solution. It is important to underline that, in this simplified case, the $\boldsymbol{K}_\sigma$ matrix refers only to the linear contribution of the stress.
These vectors and matrices are expressed in the CUF domain. According to CUF, the three-dimensional (3D) displacement field in the dynamic case for a generic composite 1D/2D model, represented using a Cartesian system (*x*, *y*, *z*), is defined as a general expansion of the primary unknowns:

$$\begin{cases} \boldsymbol{1D}: & \boldsymbol{u}^k(x,y,z;t) = F_\tau^k(x,z)\boldsymbol{u}_\tau^k(y;t) \\ \boldsymbol{2D}: & \boldsymbol{u}^k(x,y,z;t) = F_\tau^k(z)\boldsymbol{u}_\tau^k(x,y;t) \end{cases} \qquad \tau = 1,\ldots,\mathrm{M} \tag{4}$$

in which $\boldsymbol{u}_\tau$ is the generalized displacement vector, $F_\tau$ represent the expansion functions of the thickness coordinate *z*, M denotes the order of expansion in the thickness direction, *k* indicates the

layer index in laminated composite structures and *t* stand for time.
In this research, Lagrange polynomials (LE) are adopted for the expansion functions. In the CUF domain, the nine-point (L9) Lagrange polynomials were adopted to formulate the higher-order kinematic beam model, while the three-node quadratic (LD2) Lagrange expansion was employed in the thickness direction to obtain the higher-order kinematic of the plate/shell model.
For brevity, readers are referred to [12] for a full explanation about the mathematical derivation of the 1D/2D FE formulation in the domain of CUF.
The finite element method (FEM) is used to approximate the in-plane generalized displacement vector employing the shape function $N_i$.

$$\begin{cases} \mathbf{1D}\text{: } \boldsymbol{u}_\tau^k(y;t) = N_i(y)\boldsymbol{q}_{\tau i}^k(t) \\ \mathbf{2D}\text{: } \boldsymbol{u}_\tau^k(x,y;t) = N_i(x,y)\boldsymbol{q}_{\tau i}^k(t) \end{cases} \qquad i = 1,\ldots, \mathrm{N_n} \tag{5}$$

in which $N_n$ stand for the number of nodes per element and *i* indicates summation. For clarity, the four-node (B4) cubic beam element is adopted in this work as shape function or the classical nine-node quadratic (Q9) for the plate element.
In this study, employing the total Lagrangian formulation, the full Green-Lagrange nonlinear strain vector is adopted.

$$\boldsymbol{\varepsilon}^k = \boldsymbol{\varepsilon}_l^k + \boldsymbol{\varepsilon}_{nl}^k = (\boldsymbol{b}_l + \boldsymbol{b}_{nl})\boldsymbol{u}^k \tag{6}$$

where $\boldsymbol{b}_l$ and $\boldsymbol{b}_{nl}$ represent the linear and nonlinear differential operators [13].
The stress vector is computed from the constitutive relation:

$$\boldsymbol{\sigma}^k = \boldsymbol{C}^k\boldsymbol{\varepsilon}^k \tag{7}$$

in which $\boldsymbol{C}$ is the material elastic matrix for orthotropic materials and it is defined in [14].
Considering the linear thermo-elasticity, the elastic strain vector $\boldsymbol{\varepsilon}_e^k$ is equal to:

$$\boldsymbol{\varepsilon}_e^k = \boldsymbol{\varepsilon}^k - \boldsymbol{\varepsilon}_T^k \tag{8}$$

where $\boldsymbol{\varepsilon}_T^k$ represents the strain vector due to the temperature change $\Delta T = T - T_0$, that is expressed as:

$$\boldsymbol{\varepsilon}_T^k = \boldsymbol{\alpha}^k \boldsymbol{\Delta T} \tag{9}$$

in which $T_0$ indicates the reference temperature and α stands for the linear thermal expansion coefficients vector.
Consequently, the introduction of the thermal contribution leads to the definition of a new constitutive law and to a component related to the thermal load ($\boldsymbol{F}_T$) in the integral of the virtual variation of the internal work and a new contribution in the geometric stiffness matrix ($\boldsymbol{K}_{\sigma_T}$). For the sake of brevity, the complete description with thermal contribution is not provided here, the interested reader is referred to [15].

## 3. Numerical results

In order to show the potential of the presented approach, some results obtained based on the use of virtual VCT for metallic and composite structures are illustrated below [16,17].
For the representative purpose, different metallic plates subjected to compressive load are investigated as first example. In detail, one unstiffened plate and two stiffened structures are considered. These structures have the following geometrical and material data: width (*a*) equal to 355 mm, the length (*b*) is 355 mm, a total thickness (*h*) of 2 mm. The dimensions of the stiffener are: *l* = 7 mm and *d* = 4 or 7 mm, respectively. The material properties are: E = 70 GPa, υ = 0.33 and ρ = 2780 $\mathrm{kg/m^3}$. The boundary conditions of this plate are illustrated in Fig. 1.

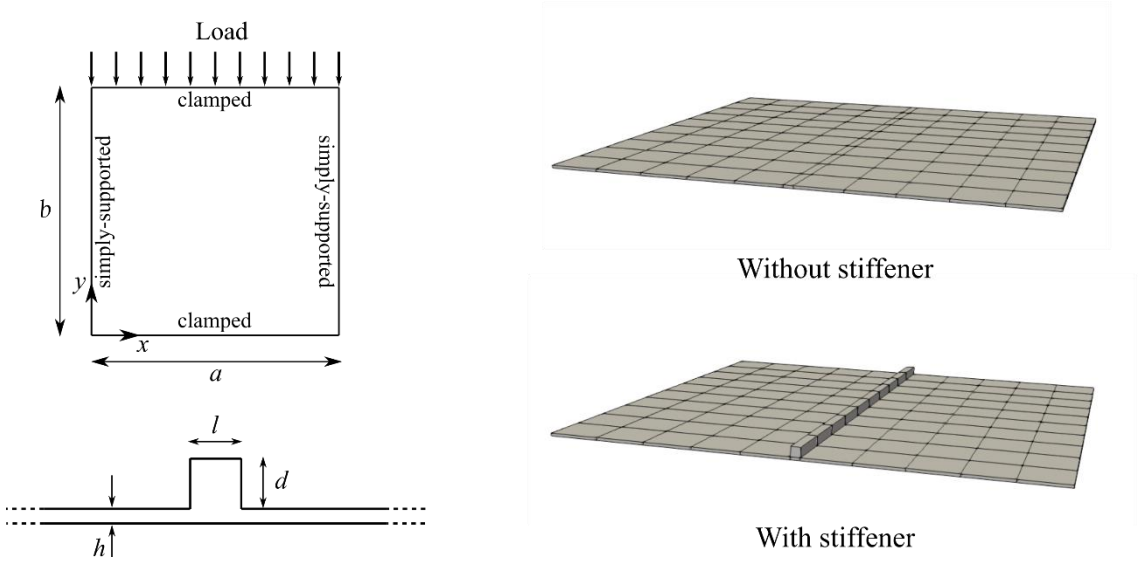


Figure 1 - Geometry and boundary conditions of the unstiffened and stiffened plate structures.

For the following discussions, the convergent model is obtained by adopting at least 11x10Q9 for the in-plane mesh approximation and only one LD2 in the thickness direction. For the stiffened structure, another LD2 is added to describe the stiffener.
Figure 2 depicts the equilibrium curves of the unstiffened and stiffened plates computed by the 2D CUF nonlinear model. Furthermore, in this figure, the linearized buckling load values, representing by the horizontal lines, are also displayed. A defect load applied in the center of the plate, $F_d$ = 0.01 N, was used in order to simulate geometrical imperfections.

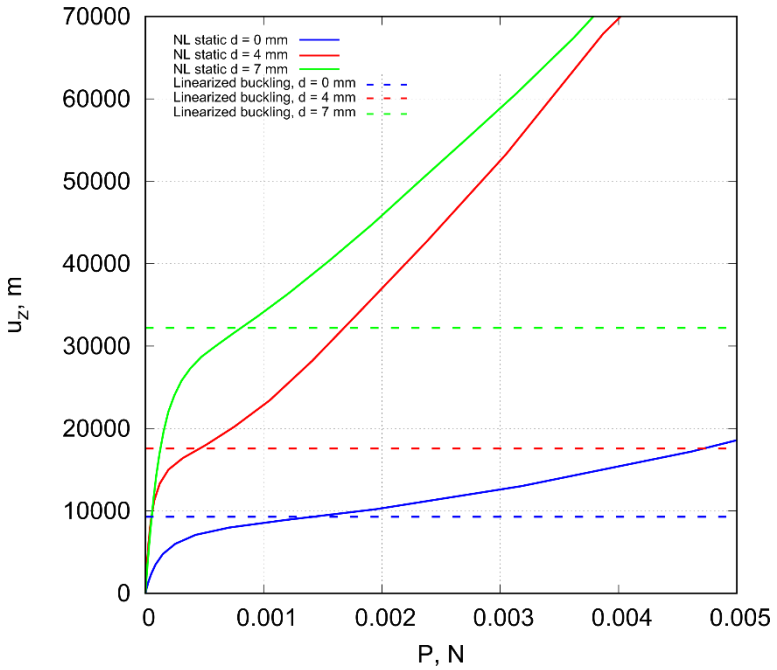


Figure 2 - Equilibrium curves for the unstiffened and stiffened plates under in-plane compressive loads. CUF model makes use of LD2 kinematics and 11x10Q9 FE mesh approximation.

Figure 3 shows the comparison between the variation of the natural frequencies for progressively increasing loads via the trivial linearized solution and full nonlinear approach for the three cases considered. For completeness the first ten free vibration modes shapes for the stiffened plate with *d* = 7 mm are reported in Fig. 4.

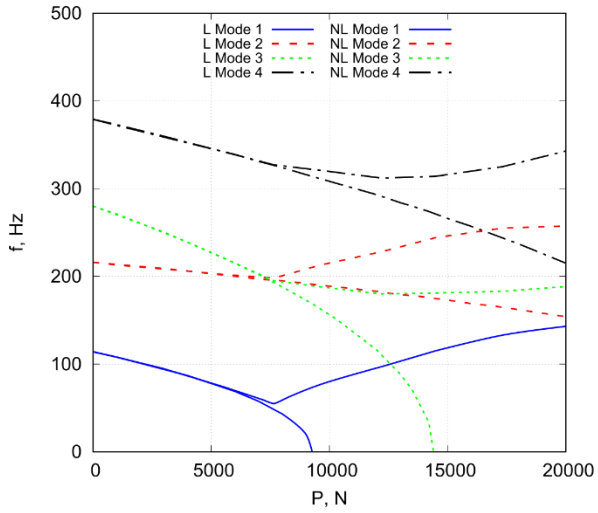


(a) $d = 0$ mm

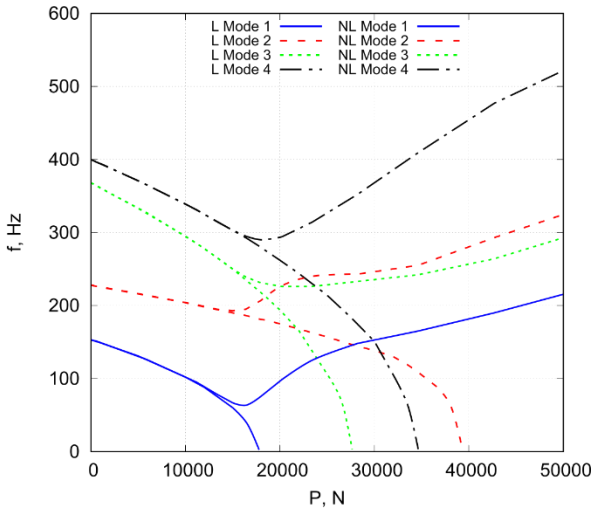


(b) $d = 4$ mm

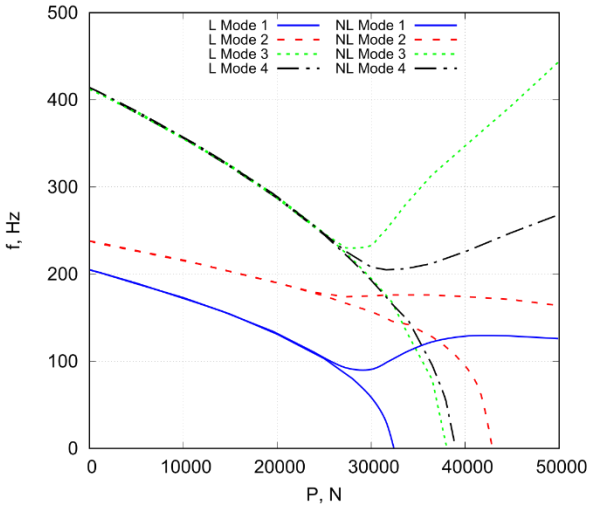


(c) $d = 7$ mm

Figure 3 - Comparison between the natural frequencies variation versus compressive loading via the trivial linearized solution (L) and full nonlinear approach (NL) for the (a) unstiffened plate, (b) stiffened plate with $d$ = 4 mm and (c) stiffened plate with $d$ = 7 mm.

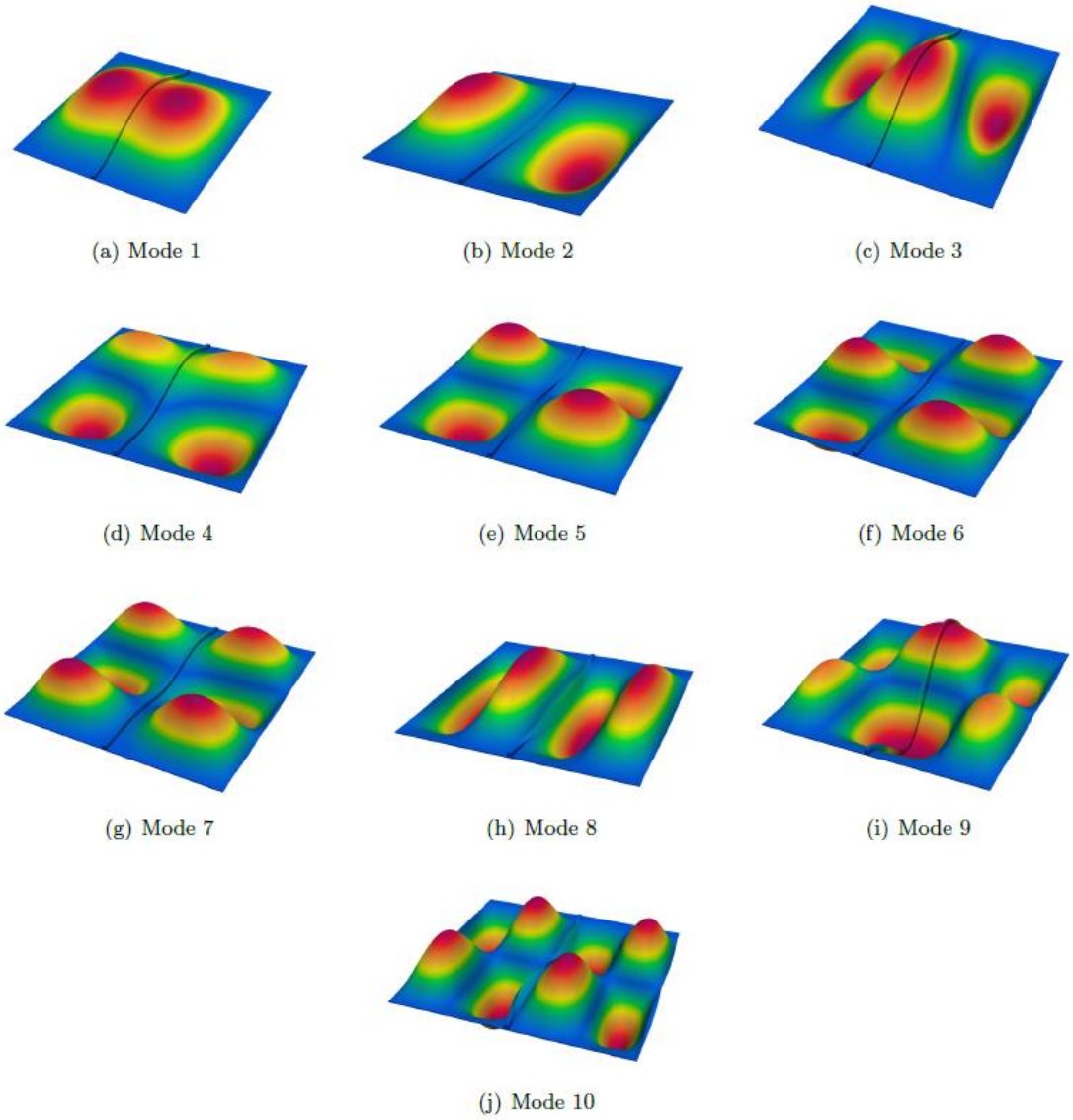


Figure 4 - Characteristic first ten free vibration mode shape for the stiffened plate structures with *d* = 7 mm.

The results show that the approach based on the trivial linearized solution allows one to evaluate the frequency variation of this case at lower levels of the compressive load with accuracy. The deviation of the linear results from the nonlinear ones becomes remarkable for higher compressive load levels. In detail, the first vibration mode reaches a minimum value near the critical load, and after the buckling, the frequencies increase. This definite change in the slope of the frequencies represents a criterion for the buckling prediction. The results suggest that the proposed methodology provides an excellent procedure to predict the critical load and to evaluate the natural frequencies variation in nonlinear regime with high reliability. In addition, the presented approach allows to model the structure with high accuracy and also take into account the deformation of the stiffener, as illustrated in Fig. 4. For completeness, a Modal Assurance Criterion (MAC) graphical representation is reported in Fig. 5. This figure compares the first 10 modes of the deformed structure in different states of the nonlinear analysis with the undeformed one. As reported by these graphical representations, natural modes for a low load (Fig. 5a) are identical to those related to the undeformed case; i.e., all the MAC values in the diagonal are equal to 1. As the load increases, more and more boxes are different from 1 and the state is entirely nonlinear.

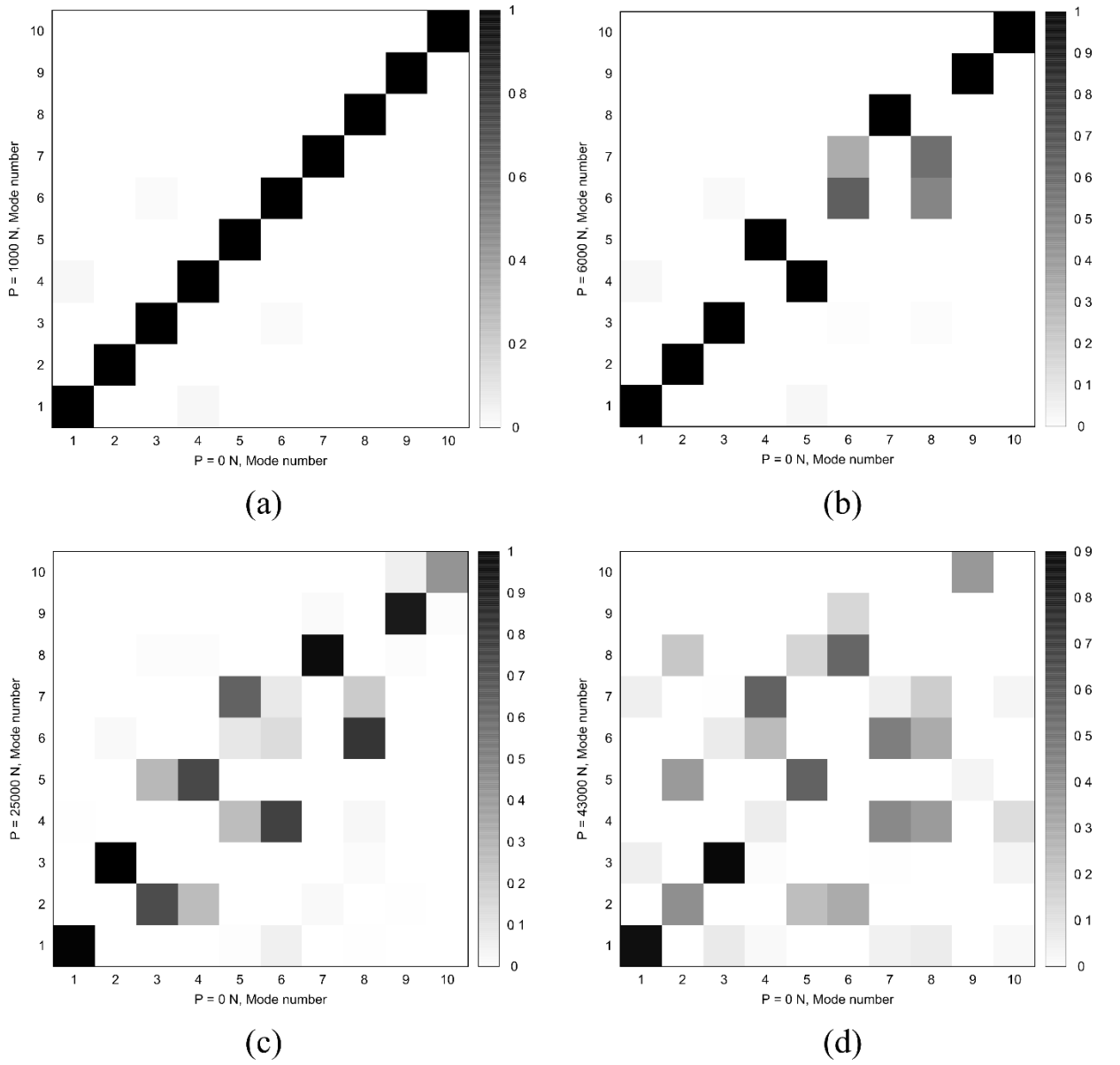


Figure 5 - MAC values between the modes of the undeformed structure and those of the deformed structure for the stiffened plate with *d* = 4 mm.

A 3-layer [90°+<0°/45°> / 0°+<0°/45°> / 90°+<0°/45°>] hinged variable angle tow (VAT) composite shell subjected to in-plane compressive and transverse load is illustrated as second assessment. This structure has the following data: L = 508 mm, $R_\alpha$ = 2540 mm, θ = 0.1 rad, h = 12.7 mm, $E_1$ = 3300 MPa, $E_2$ = $E_3$=1100 MPa, $G_{12}$ = $G_{13}$ = 660 MPa, $\upsilon_{12}$ = $\upsilon_{13}$ = 0.25, ρ = 1 kg/mm$^3$. All nodal displacements are restrained along the hinged edges, see Fig. 3. The present shell is modelled adopting 10x10Q9 for the in-plane mesh approximation and one LD2 in each layer in the *z*-direction. The equilibrium curves of the considered shell structure are provided in Fig. 6.

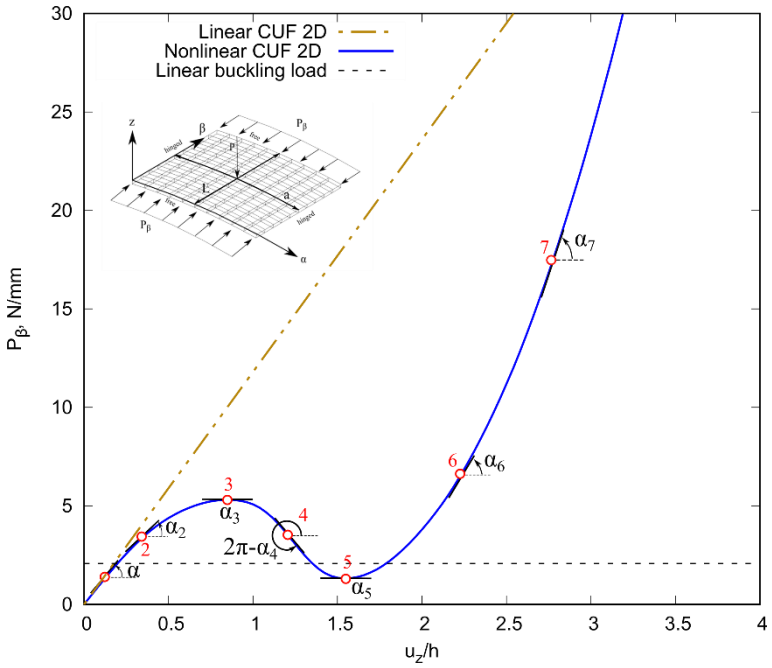


Figure 6 - Equilibrium curves evaluated at the center of the hinged VAT composite shell under compressive and transverse loads.

Figure 7 illustrates the comparison between the first two natural frequencies variation obtained via the trivial linearized solution and the full nonlinear approach. In this figure, the red dots and the relative numbers refer to those displayed in Fig. 6. The results prove that for this type of structure to evaluate the trend of the natural frequencies accurately is needed to perform a nonlinear analysis.

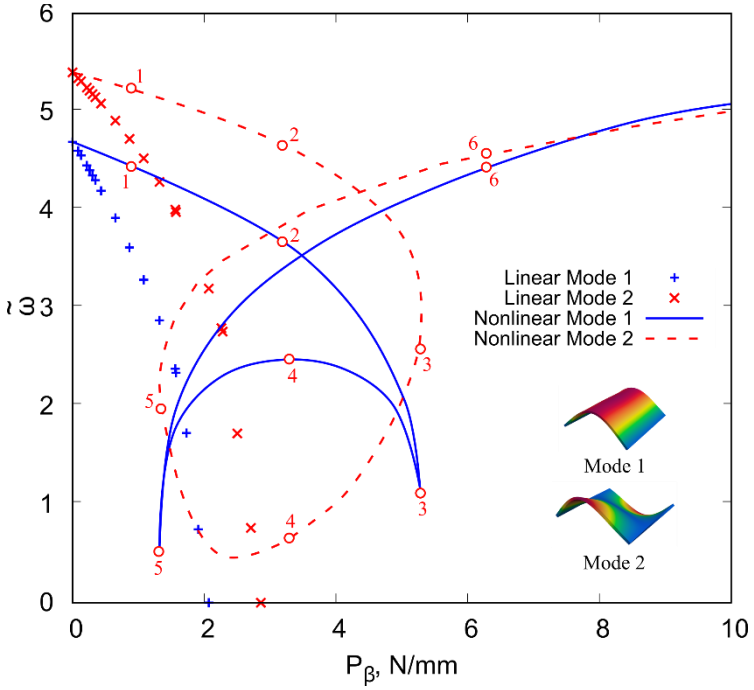


Figure 7 - Comparison between the approach based on trivial linearized solution and full nonlinear solution for the variation of the first two non-dimensional natural frequencies for the hinged VAT composite shell subjected to compressive and transverse loads. $\left(\tilde{\omega} = \omega\left(\frac{a^2}{h}\sqrt{\frac{\rho}{E_2}}\right)\right)$

As a final example, a clamped-clamped laminated composite [0°/90°/0°] beam structures subjected to thermal loadings is analyzed, see Fig. 8b. The geometrical and material properties are: L = 1 m,

a = 0.01 m, h = 0.01 m, $E_1$ = 144.8 GPa, $E_2 = E_3$ = 9.65 GPa, $\nu_{12}$ = 0.3, $G_{12} = G_{13}$ = 4.14 GPa, $G_{23}$ = 3.45 GPa, ρ = 1450 kg/m$^3$, $\alpha_{11} = -2.6279\text{x}10^{-7}$ °$C^{-1}$ and $\alpha_{12} = 30.535\text{x}10^{-6}$ °$C^{-1}$. The convergent model for this beam structure is reached by using at least ten B4 FE along the beam axis and two Q9 for each layer.
In Fig. 8a the comparison between the natural frequencies variation for progressively increasing thermal loadings computed via the presented trivial linearized approach and Abaqus (Hex20). For completeness, the first four free vibration mode shapes of the composite beam are depicted in Fig. 8c, 8d, 8e, 8f.

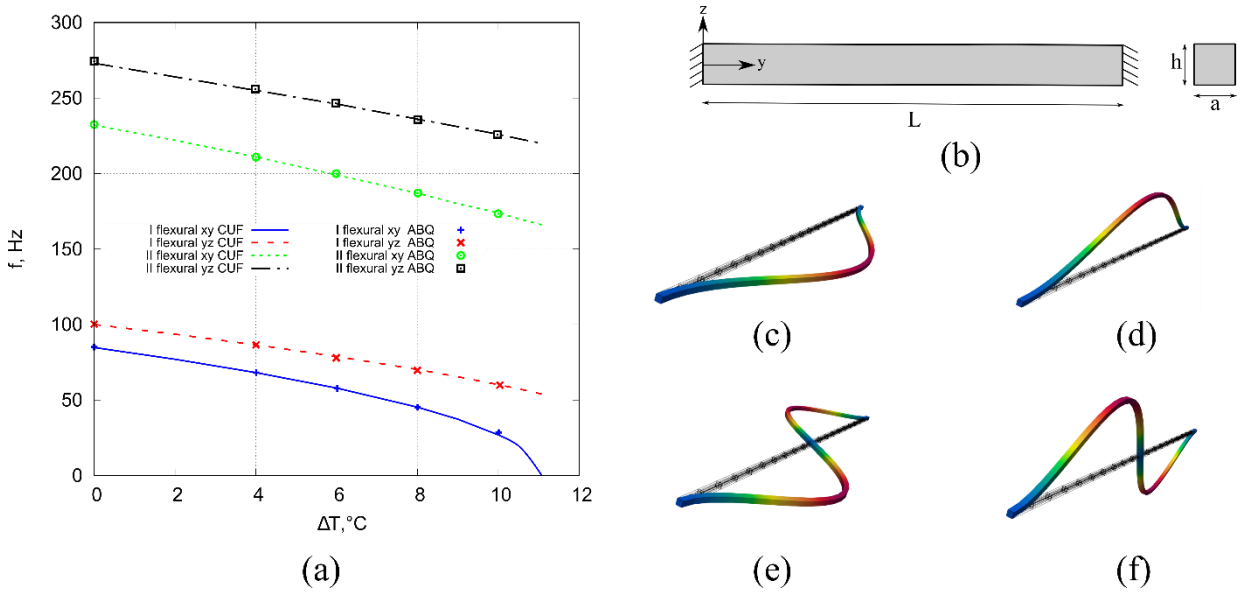


Figure 8: (a) Natural frequencies variation versus thermal loadings for the composite beam; (b) Geometry and boundary conditions; (c) I flexural xy mode; (d) I flexural yz mode; € II flexural xy mode; (f) II flexural yz mode.

## 4. Concluding remarks

The presented method allows to determine the buckling load of metallic and composite unstiffened and stiffened structures subjected to mechanical and thermal loadings, to evaluate the natural frequencies variation and to provide a verification of the experimental VCT results with high reliability. Furthermore, the virtual VCT becomes a useful technique during the preparation of the experimental test or a powerful method when it is necessary to investigate cases that are difficult to analyze experimentally, such as structures subjected to thermal or shear loads and with complicated boundary conditions, among others. The results demonstrated the potential of this approach and provide reasonable confidence for future applications in this topic. In detail, a full nonlinear approach is needed to perform accurate investigations. It was shown that eigenfrequencies and eigenmodes can suffer abrupt aberrations in deep nonlinear regimes. Moreover, mode aberration is evident compared to the modes calculated using the full nonlinear approach with those obtained using the trivial linearized solution.

## 5. Contact Author Email Address

*e-mail address of the corresponding author: *rodolfo.azzara@polito.it*

## 6. Copyright Statement

## References


[1] J. Singer, J., Arbocz. T. Weller. Buckling Experiments: Experimental Methods in Buckling of Thin-Walled Structure, Vol. 1: Basic Concepts, Columns, Beams and Plate. *John Wiley & Sons Inc.*, New York, USA (1998)

[2] J. Singer, J., Arbocz. T. Weller. Buckling Experiments: Experimental Methods in Buckling of Thin-Walled Structure, Vol. 2: Shells, Built-up Structures and Additional Topics. *John Wiley & Sons Inc.*, New York, USA (2002)

[3] H. Lurie. Lateral vibrations as related to structural stability. *Journal of Applied Mechanics, ASME,* **19**, pp. 195-204 (1950)

[4] J.H. Meier. The determination of critical load of a column or stiffened panel in compression by the vibration method. *Proceeding of the Society for Experimental Stress analysis*, Volume **11** (1953).

[5] T.H. Chu. Determination of buckling loads by frequency measurements. *PhD thesis, California Institute of Technology* (1949).

[6] H. Abramovich, D. Govich, A. Grunwald. Buckling prediction of panels using the vibration correlation technique. *Progress in Aerospace Sciences,* **78**, pp. 62-73 (2015)

[7] E. Jansen. H, Abramovich, R. Rolfes. The direct prediction of buckling loads of shells under axial compression using VCT-towards an upgraded approach. *29th Congress on the Internal Council of the Aeronautical Science*, pp. 1-9 (2014)

[8] E. Skukis, O. Ozolins, J. Anderson, K. Kalnins, M. Arbelo. Applicability of the Vibration Correlation Technique for estimation of the buckling load in axial compression of cylindrical isotropic shells with and without circular cutouts. *Shock and Vibration* (2017).

[9] E. Carrera, A. Pagani, R. Azzara, R. Augello. Vibration of metallic and composite shells in geometrical nonlinear equilibrium states. *Thin-Walled Structures*, **157**, pp. 101-131 (2020).

[10] S. Samukham, G. Raju, C.P. Vyasarayani, P.M. Weaver Dynamic instability of curved variable angle tow composite panel under axial compression. *Thin-Walled Structures*, **138**, pp. 302-312 (2019).

[11] P. Ribeiro, H. Akhavan. Nonlinear vibrations of variable stiffness composite laminated plates. *Composite Structures*, **95(8)**, pp. 2424-2432 (2012).

[12] E. Carrera, M. Cinefra, M. Petrolo, E. Zappino. Finite Element Analysis of Structures through Unified Formulation. *John Wiley & Sons*, West Sussex, UK (2014).

[13] E. Carrera, A. Pagani, R. Augello, B. Wu. Popular benchmarks of nonlinear shell analysis solved by 1D and 2D CUF-based finite elements. *Mechanics of Advanced Materials and Structures*, pp. 1-12 (2020).

[14] K.J. Bathe. Finite element procedure. *Prentice Hall*, Upper Saddle River, New Jersey, USA (1996).

[15] R. Azzara, E. Carrera, M. Filippi, A. Pagani. Vibration analysis of thermally-loaded isotropic and composite beam and plate structures. submitted.

[16] R. Azzara, E. Carrera, A. Pagani. Nonlinear and linearized vibration analysis of plates and shells subjected to compressive loading. *International Journal of Non-Linear Mechanics*, 141 (2022): 103936.

[17] A. Pagani. R. Azzara, E. Carrera. Geometrically nonlinear analysis and vibration of in-plane-loaded variable angle tow composite plates and shells. *Acta Mechanica*, 1-24 (2022)